Optimal Sensor Placement for Multilateration Using Alternating Greedy Removal and Placement

Daniel Frisch, **Kailai Li**, and **Uwe D. Hanebeck**
Intelligent Sensor-Actuator-Systems Laboratory (ISAS)
Institute for Anthropomatics and Robotics
Karlsruhe Institute of Technology (KIT), Germany
daniel.frisch@ieee.org, kailai.li@kit.edu, uwe.hanebeck@ieee.org

***Abstract*—We present a novel algorithm for optimal sensor placement in multilateration problems. Our goal is to design a sensor network that achieves optimal localization accuracy anywhere in the covered region. We consider the discrete placement problem, where the possible locations of the sensors are selected from a discrete set. Thus, we obtain a combinatorial optimization problem instead of a continuous one. While at first, combinatorial optimization sounds like more effort, we present an algorithm that finds a globally optimal solution surprisingly quickly.**

***Index Terms*—Multilateration, Dilution of Precision, Fisher Information, Sensor Placement, Combinatorial Optimization, Greedy Algorithm.**

I. Introduction

A. Context

Multilateration (MLAT) is a popular method to localize cooperative targets. It is used on a large scale (wide-area MLAT) for air traffic localization in traditional secondary surveillance radar (SSR) [1], [2], and can also be used to verify the aircraft's self-localization transmitted via automatic dependent surveillance – broadcast (ADS-B) [3], [4]. MLAT is furthermore applied on a small scale for indoor localization. Either way, targets send out a radio signal, the time of arrival (TOA) of which is precisely measured at each of the receivers. Based on these TOAs, the MLAT algorithm computes the target location. Alternative localization methods include received signal strength (RSS) [5] and angle of arrival (AOA) [6], [7, Sec. V.A], [8]. MLAT achieves much better localization accuracy than RSS and AOA – but only if certain constraints are carefully met. These include a precise time synchronization between sensors, a unique and high-bandwidth radio signal to allow accurate TOA determination, direct line of sight between a certain number of sensors and the target, and a good choice of the installation locations of the receivers. However, there are methods that can still localize with unsynchronized sensors [9], [10], [11], with ambiguous radio signals [12], or under non-line-of-sight (NLOS) conditions [13].

B. Considered Problem

In this work, we focus on finding an arrangement of sensors (sometimes called receivers, satellites, nodes, anchors, base stations, ground stations, or transceiver stations) that facilitate optimal location accuracy in a given limited area. In wide-area MLAT systems, there is usually a discrete set of suitable locations where installation of an MLAT sensor comes into question, ideally exposed locations (enabling direct line of sight in a wide range) with existing power supply and network connection that can be rented for installation of the equipment. Typical examples are roofs of skyscrapers, television towers, hilltops, etc. Thus, we naturally face a discrete set of possible installation sites. In indoor applications, one is typically less restricted in the placement of sensors. In this case, we propose to discretize the area of interest by using a grid.

C. State of the Art

Sensor positioning for covering an extended region of interest (ROI) can be a complicated problem where no closed-form solution exists. If sensors can be freely placed to optimally localize targets at one specific position, equilateral polygons (symmetrically around the target) are the optimal choice on the plane [14] and platonic solids in the space [15]. Yet usually an extended area rather than a single spot should be covered by a multilateration system. The localization accuracy can be evaluated and averaged on a grid covering the area of interest, yielding a scalar objective function, and the wanted sensor locations can be obtained via nonlinear optimization methods [16]. Alternatively, instead of optimizing the average localization accuracy in the area of interest, the worst accuracy can be optimized, yielding two concatenated optimization problems [17]. Now sensors can often not be freely placed, and a set of possible sites is given. The resulting sensor selection out of a discrete set of locations is a non-smooth and non-convex problem. A non-optimal solution can be found via relaxation [18] or greedy selection [19].

D. Challenges

We aim at developing an improved greedy method for computing optimal or nearly-optimal sensor configurations for passive source localization.

E. Key Idea

We propose the Alternating Greedy Removal and Placement (AGREP) algorithm. In every "placement" step, a sensor is greedily placed at the location (out of the discrete set of possible sensor locations) that maximally improves localization accuracy. In every "removal" step, a sensor is greedily removed such that the localization accuracy deteriorates the least. A random number of "placement" steps takes turns with a random number of "removal" steps, see purple line in Fig. 1. Each time we pass over the desired number of sensors, we compare the localization accuracy of the current sensor configuration with the best one we have seen so far and update the latter if necessary. This algorithm always compares sensor configurations where a single sensor is added or removed. We show that this update can be efficiently calculated using the Sherman–Morrison formula.

II. Multilateration

For a given sensor configuration (that will be altered and optimized later), the sensor infrastructure consists of sensors or satellites at known locations $\underline{s}_i \in \mathbb{R}^2,\ i \in 1, \ldots, N$. We assume they are able to localize themselves with respect to each other and synchronize their clocks. A tag (sometimes called target, moving object, aircraft, mobile station, etc.) at unknown position $\underline{p} \in \mathcal{P} \subset \mathbb{R}^2$ emits an ultra-wideband (UWB) signal at unknown transmission time t_0. The signal spreads with propagation velocity c and arrives at some of the satellites $\underline{s}_i$. The satellites measure the respective TOA t_i, subject to additive white Gaussian noise v. Therefore, we have the measurement model

$$\underline{x} = \begin{bmatrix} \underline{p} \\ t_0 \end{bmatrix} \ , \tag{1}$$

$$t_i = h_i(\underline{x}) + v_i \ , \tag{2}$$

$$h_i(\underline{x}) = c^{-1} \left\| \underline{p} - \underline{s}_i \right\| + t_0 \ . \tag{3}$$

Note that although the time difference of arrival (TDOA) measurement model seems to be more popular in literature, we use the TOA model because it gives identical results with uncorrelated v_i, making modeling and computation somewhat easier. Note also that the measurement model can be made more accurate, e.g., by introducing a distant-dependent measurement noise v_i. However, this is highly problem-specific (application scenario, sensor hardware, etc.), so we choose this simple but universal model.

Given enough measurements t_i, the target location $\underline{p}$ can be estimated using, e.g., a maximum likelihood estimator. For additive white Gaussian noise with equal variances, this simplifies to the least-squares estimator

$$\hat{\underline{x}} = \arg\min_{\underline{x}} \left\{ \sum_{i=1}^{N} \left(h_i(\underline{x}) - t_i \right)^2 \right\} \ . \tag{4}$$

This can be efficiently solved using the Levenberg-Marquardt algorithm [20], [21]. In the following, we assume that an unbiased and efficient estimator is used which thus yields the Cramér–Rao lower bound (CRLB).

III. Localization Accuracy

Estimating the tag position $\underline{p}$ from TOA measurements t_i, we get a certain localization error that is caused by the measurement error v_i. Depending on the position of the sensors and targets relative to each other, the localization error can be larger or smaller (for a fixed measurement error). We aim to find a distribution of sensors that minimize the influence of the measurement error on the localization error. For that purpose, we derive the relationship between measurement error and localization error in the following.

A. Linearization

The gradient of the measurement model (3) for an individual satellite

$$\nabla h_i = \begin{bmatrix} \frac{p^{(x)} - s_i^{(x)}}{\left\|\underline{p} - \underline{s}_i\right\|} & \frac{p^{(y)} - s_i^{(y)}}{\left\|\underline{p} - \underline{s}_i\right\|} & 1 \end{bmatrix}^\top \tag{5}$$

contains the "direction cosines" from tag to satellite, and the Jacobian for all visible satellites

$$\mathbf{H} = \begin{bmatrix} \nabla h_1^\top \\ \vdots \\ \nabla h_N^\top \end{bmatrix} = \begin{bmatrix} \frac{p^{(x)} - s_1^{(x)}}{\left\|\underline{p} - \underline{s}_1\right\|} & \frac{p^{(y)} - s_1^{(y)}}{\left\|\underline{p} - \underline{s}_1\right\|} & 1 \\ \frac{p^{(x)} - s_2^{(x)}}{\left\|\underline{p} - \underline{s}_2\right\|} & \frac{p^{(y)} - s_2^{(y)}}{\left\|\underline{p} - \underline{s}_2\right\|} & 1 \\ \vdots & \vdots & \vdots \\ \frac{p^{(x)} - s_N^{(x)}}{\left\|\underline{p} - \underline{s}_N\right\|} & \frac{p^{(y)} - s_N^{(y)}}{\left\|\underline{p} - \underline{s}_N\right\|} & 1 \end{bmatrix} . \tag{6}$$

Using the differential measurement model

$$\Delta \underline{t} = \mathbf{H} \, \Delta \underline{x} \ , \tag{7}$$

we can relate the covariance $\mathbf{C}^v$ of the measurement error v and the covariance $\mathbf{C}^x$ of the unknown parameters

$$\mathbf{C}^v = \mathbf{H} \, \mathbf{C}^x \, \mathbf{H}^\top \ , \tag{8}$$

$$\mathbf{C}^x = \left(\mathbf{H}^\top \left(\mathbf{C}^v \right)^{-1} \mathbf{H} \right)^{-1} \ , \tag{9}$$

$$\mathbf{J}^x = \mathbf{H}^\top \mathbf{J}^v \, \mathbf{H} \ , \tag{10}$$

with the Fisher information matrix (FIM) $\mathbf{J} = \mathbf{C}^{-1}$. For $\mathbf{J}^v = \mathbf{I}$, we obtain

$$\mathbf{J}^x = \mathbf{H}^\top \mathbf{H} \tag{11}$$

$$= \sum_{i=1}^{N} \nabla h_i \left[\nabla h_i \right]^\top \ , \tag{12}$$

thus every satellite contributes an individual satellite information matrix

$$\mathbf{J}_i^x = \nabla h_i \left[\nabla h_i \right]^\top \tag{13}$$

$$= \begin{bmatrix} \left(\frac{p^{(x)} - s_i^{(x)}}{\left\|\underline{p} - \underline{s}_i\right\|} \right)^2 & \frac{p^{(x)} - s_i^{(x)}}{\left\|\underline{p} - \underline{s}_i\right\|} \cdot \frac{p^{(y)} - s_i^{(y)}}{\left\|\underline{p} - \underline{s}_i\right\|} & \frac{p^{(x)} - s_i^{(x)}}{\left\|\underline{p} - \underline{s}_i\right\|} \\ \frac{p^{(x)} - s_i^{(x)}}{\left\|\underline{p} - \underline{s}_i\right\|} \cdot \frac{p^{(y)} - s_i^{(y)}}{\left\|\underline{p} - \underline{s}_i\right\|} & \left(\frac{p^{(y)} - s_i^{(y)}}{\left\|\underline{p} - \underline{s}_i\right\|} \right)^2 & \frac{p^{(y)} - s_i^{(y)}}{\left\|\underline{p} - \underline{s}_i\right\|} \\ \frac{p^{(x)} - s_i^{(x)}}{\left\|\underline{p} - \underline{s}_i\right\|} & \frac{p^{(y)} - s_i^{(y)}}{\left\|\underline{p} - \underline{s}_i\right\|} & 1 \end{bmatrix} .$$

The overall information matrix $\mathbf{J}^x$ at a given location $\underline{p}$ is simply the sum of those "satellite information matrices" where satellites have a direct line of sight to $\underline{p}$.

Note that we describe the method based on the two-dimensional localization problem for ease of notation and visualization, to communicate the basic concept as intuitively as possible. The generalization to three-dimensional geometries is straightforward.

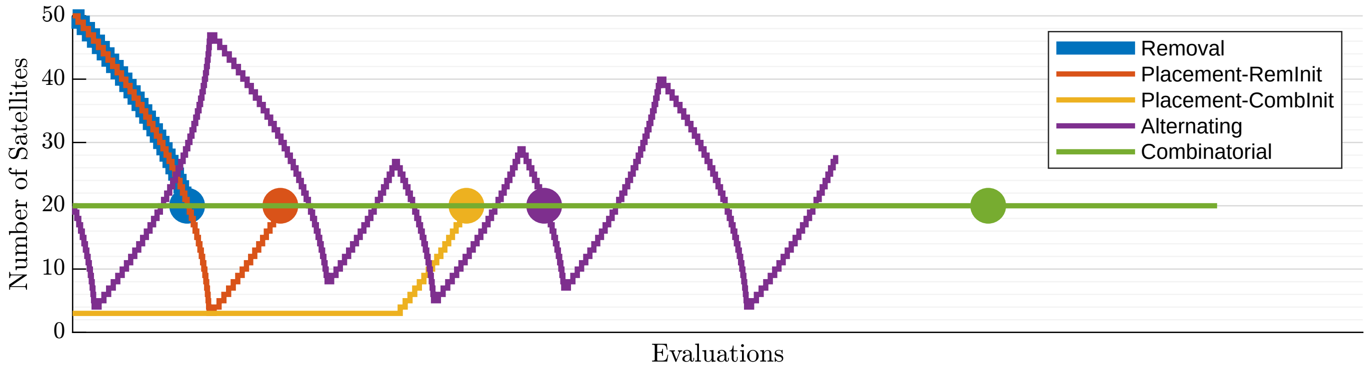

Fig. 1: Exemplary representation of different search routines. There are $M = 50$ potential satellite locations where $N = 20$ satellites should be optimally placed. Greedy removal (blue) starts with a fully occupied satellite grid (50 sensors) and consecutively removes the least important sensor until the desired 20 sensors are left. Greedy placement starts with a minimal configuration (3 sensors in 2D) that is itself obtained either by greedy removal (orange) or combinatorial search (yellow) and subsequently adds sensors at the most profitable locations. Greedy alternating (purple) combines greedy removal and greedy placement randomly. Combinatorial search (green) considers all the possible combinations of 20 sensors. The point where any method finds its final result is indicated by a dot. Note that the horizontal axis represents the number of rank-1 update evaluations as well as computation time, but it is not quite to scale for better visualization, therefore printed without scale.

B. Information Metric

Now we need an information metric that summarizes the FIM to a scalar value. Doing this for every point $\underline{p}$ in space, we obtain a scalar field. This has been called the Fisher information field (FIF) [22, Sec. 6.A.1]. The most straightforward information metric is the trace of the FIM, also termed T−optimality. While this metric has been successfully applied in [22, Sec. 6.A.2], it is unfortunately not applicable to our case as the trace of our FIM (13) is constant. This is typical for the trace criterion, as described in [23, Sec. 6.5]. Therefore, we resort to the average-variance criterion, i.e., the trace of the inverse of the FIM [23, Sec. 6.5]. Summarizing, we are back to (9) or

$$\mathbf{C}^x = \left(\mathbf{H}^\top \mathbf{H}\right)^{-1} \tag{14}$$

in case of independent and identically distributed standard normal measurement noise. In the areas where targets are to be localized, $\mathrm{trace}(\mathbf{C}^x)$ should be as small as possible [24, Eq. 15]. This value is very important to characterize MLAT systems and is called the geometric dilution of precision (GDOP).

C. Gradient Descent

In a simple setup without occlusions, as considered here, the cost function $\mathrm{trace}(\mathbf{C}^x)$ is smooth and the problem can be solved with gradient descent or Newton-like optimization methods. However, keeping open the possibility of extension to more complex scenarios with non-smooth cost functions in future works, we do not consider this path further here. Also, the set of potential sensor locations is often a discrete set of points by nature due to spatial and organizational restrictions, and gradient descent methods are unsuitable for such constraints.

D. Rank-One Update

As the trace of the inverse matrix is not a linear measure, it is not possible to quantify the gain to the overall localization accuracy from all individual satellites independently. We can only quantify the additional localization gain $\delta\mathbf{C}^x_{\mathbf{H}\cup i}$ for an individual satellite $\underline{s}_i$ starting from a certain arrangement of the *other* satellites (encoded in $\mathbf{H}$)

$$\begin{aligned} \mathbf{C}^x_{\mathbf{H}\cup i} &= \left(\mathbf{H}^\top \mathbf{H} + \mathbf{J}^x_i\right)^{-1} && (15) \\ &= \mathbf{C}^x_{\mathbf{H}} + \delta\mathbf{C}^x_{\mathbf{H}\cup i} && (16) \\ &= \mathbf{C}^x_{\mathbf{H}} - \frac{\mathbf{C}^x_{\mathbf{H}} \nabla h_i \left[\mathbf{C}^x_{\mathbf{H}} \nabla h_i\right]^\top}{1 + \left[\nabla h_i\right]^\top \mathbf{C}^x_{\mathbf{H}} \nabla h_i} && (17) \end{aligned}$$

with the simplification according to the Sherman–Morrison formula [25]. The increment in our scalar metric, the trace of the covariance matrix, is therefore

$$\mathrm{trace}(\mathbf{C}_{\mathbf{H}\cup i}) = \mathrm{trace}(\mathbf{C}^x_{\mathbf{H}}) - \frac{\|\mathbf{C}^x_{\mathbf{H}} \nabla h_i\|_2^2}{1 + \left[\nabla h_i\right]^\top \mathbf{C}^x_{\mathbf{H}} \nabla h_i} \ . \tag{18}$$

For removing satellite $\underline{s}_i$ from an arrangement, we have

$$\mathbf{C}_{\mathbf{H}\setminus i} = \mathbf{C}^x_{\mathbf{H}} + \frac{\mathbf{C}^x_{\mathbf{H}} \nabla h_i \left[\mathbf{C}^x_{\mathbf{H}} \nabla h_i\right]^\top}{1 - \left[\nabla h_i\right]^\top \mathbf{C}^x_{\mathbf{H}} \nabla h_i} \ , \tag{19}$$

$$\mathrm{trace}(\mathbf{C}_{\mathbf{H}\setminus i}) = \mathrm{trace}(\mathbf{C}^x_{\mathbf{H}}) + \frac{\|\mathbf{C}^x_{\mathbf{H}} \nabla h_i\|_2^2}{1 - \left[\nabla h_i\right]^\top \mathbf{C}^x_{\mathbf{H}} \nabla h_i} \ . \tag{20}$$

IV. Sensor Placement

For optimal sensor placement, we need to optimize the N sensor positions $\underline{s}_i$ such that an objective function, e.g., one of

$$\Theta(\underline{s}_1, \ldots, \underline{s}_N) = \int_{\mathcal{P}} \mathrm{trace}(\mathbf{C}^x)\, \mathrm{d}\underline{p} \ , \tag{21}$$

$$\Theta(\underline{s}_1, \ldots, \underline{s}_N) = \max_{\underline{p} \in \mathcal{P}} \{\mathrm{trace}(\mathbf{C}^x)\} \ , \tag{22}$$

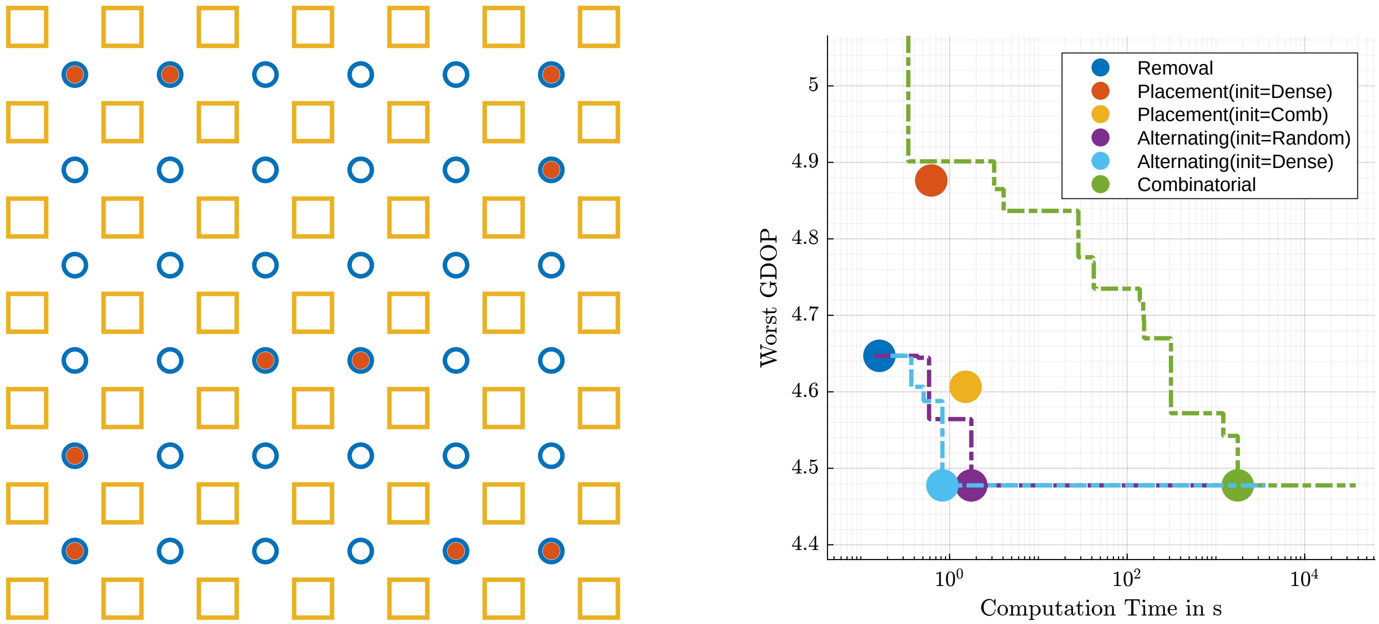

(a) Geometry

(b) Convergence

Fig. 2: (a) Geometry with $M = 36$ potential satellite voxels (blue circles) and 49 discretized target locations (yellow boxes). The optimal sensor arrangement of $N = 10$ sensors is indicated by red dots. (b) Convergence of the various search routines. The global optimum is found via the greedy alternating search as well as the combinatorial search.

is minimized. The problem here is that the objective function value itself is not easy to calculate. Therefore, we discretize the potential target locations $\underline{p} \in \mathcal{P}$ as well as the potential sensor locations $\underline{s}_i$ into a voxel grid. Then, there is a finite set of intermediate results that can be pre-computed to avoid redundant computations [22]. Note that if a mean measure (21) is used, this can often lead to "blind spots" with high localization error [17]. Thus, in the following, we optimize the localization accuracy at the worst point,

$$\hat{\underline{p}} = \max_{\underline{p} \in \mathcal{P}} \{\text{trace}(\mathbf{C}^x)\} \quad , \tag{23}$$

so that in the whole covered area at least the corresponding accuracy is achieved. Only if multiple sensor configurations have the same accuracy at the worst point will we consider the average localization accuracy to compare them.

A. Combinatorial Search

There are $\binom{M}{N}$ combinations to place N satellites at M potential satellite positions or satellite voxels. The global optimum of the discretized problem can be determined by iterating through all these combinations. Of course this is feasible only for a limited number of voxels M, as the computational complexity is about $\mathcal{O}(\binom{M}{N})$. There are "Gray code" enumerations for combinations [26, Sec. 4], where two consecutive combinations differ only in two places (one sensor added and one removed). Thus, we may benefit from the rank-one update of the covariance matrix (18).

B. Greedy Removal

Much more efficient than combinatorial search is greedy sensor removal. We initialize with fully occupied satellite voxels ($N = M$). Then we quantify how much the FIF would degrade if any single satellite would be removed, and ultimately remove the satellite with the least effect on the FIF. We continue this process until the desired number of satellites N is achieved. Computational complexity is $\mathcal{O}(M \cdot (M - N))$. The effect of removing a single satellite can be efficiently calculated with (18), effectively reducing the constant factor of the computational complexity.

C. Greedy Placement

Alternatively, we can initialize with a small sensor arrangement, where one satellite at a time is added such that the positive effect on the FIF is maximized, respectively. Once a satellite is placed, its location stays fixed. The initial configuration must contain three sensors in two dimensions or four sensors in three dimensions, otherwise, the covariance is unbounded. The initial sensor locations may be obtained via combinatorial search, by greedy removal, or chosen heuristically, e.g., the corners of the room. Computational complexity is $\mathcal{O}(MN)$, in addition to finding the initial configuration. This method is similar to the one described in [19].

D. Alternating Greedy Removal and Placement (AGREP)

In practice, it seems advantageous to combine greedy removal and greedy placement. We may start off with, e.g., fully occupied satellite voxels, or some random combination. Then, we perform greedy removal, where the (intermediate) target number of satellites $\tilde{N}$ is chosen randomly such that $4 \leq \tilde{N} \leq N$. Afterward, we perform greedy placement with $N \leq \tilde{N} \leq M$. Whenever we cross over the desired final number of samples N, the FIF of the current sensor arrangement is stored and the best one out of them is returned. There is no natural endpoint to this routine, it can be kept running until the best-found arrangement does not improve furthermore for some time. See Fig. 1 for a visualization of the course of action of the different search routines.

If the number of sensors N to be installed is not fixed beforehand, then simply "track" more than one number of sensors in the way described above, i.e., if any of the possible numbers of sensors is crossed, the new best arrangement for the respective N is stored.

V. Evaluation

We consider a simple two-dimensional example under line-of-sight (LOS) conditions, i.e., no obstacles. A discrete set of potential locations for satellites as well as target positions are chosen, see Fig. 2a. Objective function is the worst GDOP of all target positions, and if these are equal, we compare the mean GDOP. The sensor deployment is optimized using the strategies outlined in Sec. IV. The achieved value of the objective function over the computation time (single-threaded Matlab code on server with $2.1\,\mathrm{GHz}$ Intel Xeon Gold 6230, $7\,\mathrm{GB}$ RAM used) is shown in Fig. 2b. The best sensor selection yields a GDOP of 4.477 at the worst tag voxel and a mean GDOP of 1.763. The AGREP algorithm, either with random or dense initialization, yields that globally optimal result three orders of magnitude earlier than the combinatorial search. Experiments with different numbers of sensors and other two-dimensional geometric setups without occlusions yielded similar results.

Source Code with a MATLAB implementation of the proposed methods and the simulation will be published on Code Ocean, accessible from the paper's IEEE Xplore page.

VI. Conclusion

The pure greedy removal or placement algorithms are very fast and have a deterministic endpoint, but it depends on "luck" whether they find a reasonably good sensor configuration for a given setup of potential sensor voxels and target voxels. On the other hand, combinatorial searches waste a lot of computation time checking many sensor configurations that are completely unreasonable. However, the proposed *Alternating Greedy Removal and Placement* algorithm finds optimal or nearly optimal sensor configurations surprisingly fast. According to Fig. 2b, an optimal result was found after $0.8\,\mathrm{s}$ and $1.8\,\mathrm{s}$ using AGREP, versus $30\,\mathrm{min}$ with with a full combinatorial search.

In future work, we will apply this method to more complex situations from L-shaped areas up to a realistic, complex three-dimensional indoor localization scenario in an Industry 4.0 application, also considering NLOS conditions. Because the corresponding cost function will then no longer be smooth, our discrete approach could fully leverage its advantages. Furthermore, we will take into account more realistic measurement models, introducing range-dependent measurement noise and probability of detection (POD), and other constraints such as redundancy.

Acknowledgment

This work is supported by the German Federal Ministry of Education and Research (BMBF) under grant POMAS: Pose Estimation and Mapping Using Heterogeneous Sensor Networks (FKZ 01IS17042).

References

[1] D. Fränken and A. Hüpper, "Aircraft Positioning with Secondary Surveillance Radar and Time Of Arrival Measurements," in *2013 14th International Radar Symposium (IRS)*, vol. 1, 2013, pp. 355–360.

[2] F. Beutler and U. D. Hanebeck, "A Two-Step Approach for Offset and Position Estimation from Pseudo-Ranges Applied to Multilateration Tracking," in *Proceedings of the 13th International Conference on Information Fusion (Fusion 2010)*, Edinburgh, United Kingdom, Jul. 2010.

[3] B. Figuet, R. Monstein, and M. Felux, "Combined Multilateration with Machine Learning for Enhanced Aircraft Localization," *Proceedings*, vol. 59, no. 1, 2020. [Online]. Available: https://www.mdpi.com/2504-3900/59/1/2

[4] R. Kaune, C. Steffes, S. Rau, W. Konle, and J. Pagel, "Wide Area Multilateration using ADS-B Transponder Signals," in *2012 15th International Conference on Information Fusion*, July 2012, pp. 727–734.

[5] Q. Wang, Z. Duan, X.-R. Li, and U. D. Hanebeck, "Convex Combination for Source Localization Using Received Signal Strength Measurements," in *Proceedings of the 21st International Conference on Information Fusion (Fusion 2018)*, Cambridge, United Kingdom, Jul. 2018.

[6] D. Fränken, "Filter Initialization and Batch Estimation for Tracking with Angular-Only Measurements," in *2015 18th International Conference on Information Fusion (Fusion)*, 2015, pp. 1542–1549.

[7] K. Li, D. Frisch, S. Radtke, B. Noack, and U. D. Hanebeck, "Wavefront Orientation Estimation Based on Progressive Bingham Filtering," in *Proceedings of the IEEE ISIF Workshop on Sensor Data Fusion: Trends, Solutions, Applications (SDF 2018)*, Oct. 2018.

[8] S. Radtke, K. Li, B. Noack, and U. D. Hanebeck, "Comparative Study of Track-to-Track Fusion Methods for Cooperative Tracking with Bearings-only Measurements," in *Proceedings of the 2019 IEEE International Conference on Multisensor Fusion and Integration for Intelligent Systems (MFI 2019)*, Taipei, Republic of China, May 2019.

[9] D. Frisch and U. D. Hanebeck, "ROTA: Round Trip Times of Arrival for Localization with Unsynchronized Receivers," in *Proceedings of the 22nd International Conference on Information Fusion (Fusion 2019)*, Ottawa, Canada, Jul. 2019.

[10] ——, "Commentary to: TDOA versus ATDOA for Wide Area Multilateration System," *EURASIP Journal on Wireless Communications and Networking*, vol. 2020, no. 1, p. 43, Feb. 2020. [Online]. Available: https://doi.org/10.1186/s13638-020-1656-1

[11] J. Stefanski and J. Sadowski, "TDOA versus ATDOA for wide area multilateration system," *EURASIP Journal on Wireless Communications and Networking*, vol. 2018, no. 1, p. 179, Jul 2018. [Online]. Available: https://doi.org/10.1186/s13638-018-1191-5

[12] D. Frisch and U. D. Hanebeck, "Association-Free Multilateration Based on Times of Arrival," in *Proceedings of the 2020 IEEE International Conference on Robotics and Automation (ICRA 2020)*, Virtual, May 2020.

[13] F. Packi and U. D. Hanebeck, "Robust NLOS Discrimination for Range-Based Acoustic Pose Tracking," in *Proceedings of the 15th International Conference on Information Fusion (Fusion 2012)*, Singapore, Jul. 2012.

[14] N. Levanon, "Lowest GDOP in 2-D scenarios," *IEE Proceedings - Radar, Sonar and Navigation*, vol. 147, pp. 149–155(6), June 2000. [Online]. Available: https://digital-library.theiet.org/content/journals/10.1049/ip-rsn_20000322

[15] B. Yang and J. Scheuing, “Cramer-Rao Bound and Optimum Sensor Array for Source Localization From Time Differences of Arrival,” in *Proceedings. (ICASSP ’05). IEEE International Conference on Acoustics, Speech, and Signal Processing, 2005.*, vol. 4, 2005, pp. iv/961–iv/964 Vol. 4.

[16] J. Neering, M. Bordier, and N. Maizi, “Optimal Passive Source Localization,” in *2007 International Conference on Sensor Technologies and Applications (SENSORCOMM 2007)*, 2007, pp. 295–300.

[17] J. Perez-Ramirez, D. K. Borah, and D. G. Voelz, “Optimal 3-D Landmark Placement for Vehicle Localization Using Heterogeneous Sensors,” *IEEE Transactions on Vehicular Technology*, vol. 62, no. 7, pp. 2987–2999, 2013.

[18] S. P. Chepuri and G. Leus, “Sparsity-Promoting Sensor Selection for Non-Linear Measurement Models,” *IEEE Transactions on Signal Processing*, vol. 63, no. 3, pp. 684–698, 2015.

[19] S. Rao, S. P. Chepuri, and G. Leus, “Greedy Sensor Selection for Non-Linear Models,” in *2015 IEEE 6th International Workshop on Computational Advances in Multi-Sensor Adaptive Processing (CAMSAP)*, 2015, pp. 241–244.

[20] K. LEVENBERG, “A Method for the Solution of Certain Non-Linear Problems in Least Squares,” *Quarterly of Applied Mathematics*, vol. 2, no. 2, pp. 164–168, 1944. [Online]. Available: http://www.jstor.org/stable/43633451

[21] D. W. Marquardt, “An Algorithm for Least-Squares Estimation of Nonlinear Parameters,” *Journal of the Society for Industrial and Applied Mathematics*, vol. 11, no. 2, pp. 431–441, 1963. [Online]. Available: https://doi.org/10.1137/0111030

[22] Z. Zhang and D. Scaramuzza, “Fisher Information Field: an Efficient and Differentiable Map for Perception-aware Planning,” *arXiv:2008.03324 [cs]*, Aug. 2020, arXiv: 2008.03324. [Online]. Available: http://arxiv.org/abs/2008.03324

[23] F. Pukelsheim, *Optimal Design of Experiments*, ser. Classics in Applied Mathematics. Society for Industrial and Applied Mathematics, 1948. [Online]. Available: https://epubs.siam.org/doi/book/10.1137/1.9780898719109

[24] R. Yarlagadda, I. Ali, N. Al-Dhahir, and J. Hershey, “GPS GDOP Metric,” in *IEE Proceedings: Radar, Sonar and Navigation*, vol. 147, no. 5, 2000, pp. 259–264.

[25] J. Sherman and W. J. Morrison, “Adjustment of an Inverse Matrix Corresponding to a Change in One Element of a Given Matrix,” *The Annals of Mathematical Statistics*, vol. 21, no. 1, pp. 124–127, Mar. 1950, publisher: Institute of Mathematical Statistics. [Online]. Available: https://projecteuclid.org/journals/annals-of-mathematical-statistics/volume-21/issue-1/Adjustment-of-an-Inverse-Matrix-Corresponding-to-a-Change-in/10.1214/aoms/1177729893.full

[26] T. Mütze, “Combinatorial Gray codes – an updated survey,” 2022. [Online]. Available: https://arxiv.org/abs/2202.01280